

¹College of Chemistry and Chemical Engineering, Shanxi University, Taiyuan, China

²Modern Research Center of Traditional Chinese Medicine, Shanxi University, Taiyuan, China

³State Key Laboratory Breeding Base of Dao-di Herbs, National Resource Center of Chinese Materia Medica, China Academy of Chinese Medical Sciences, Beijing, China

⁴College of Pharmacy, Shanxi Medical University, Taiyuan, China

Involvement of C₆-volatiles in quality formation of herbal medicine:

A case study in *Astragalus membranaceus* var. *mongholicus*

Haifeng Sun^{1*}, Baoling Kang², Liping Kang³, Lanping Guo³, Huanhuan Sun⁴, Jianping Gao⁴

(Received December 22, 2016; Accepted May 8, 2017)

Summary

In this study, the effects of exogenous C₆-volatiles on *Astragalus membranaceus* var. *mongholicus* growth and secondary metabolism were explored. Five-week old seedlings of *A. membranaceus* var. *mongholicus* were exposed to different concentrations of soil-borne hexanal (10, 50, 100 μM) twice/week for 4 weeks. Non-treated plants serve as control. Growth, bioactive compounds and gene expression were measured by conventional and “omic” approaches. The results demonstrated: (1) all doses of hexanal significantly decreased chlorophyll a/b contents; (2) 10 and 100 μM hexanal significantly decreased the shoot length while 50 μM hexanal kept the value at the same level as it was in the control; (3) 50 μM hexanal effectively enhanced the contents of bioactive compounds in roots and the others had no obvious effect; (4) 50 μM hexanal induced more dysregulated metabolites in leaves than in roots, especially those associated with lipid metabolism; (5) expression of unigenes annotated as “plant-pathogen interaction”, “secondary metabolism” and “lipid metabolism” were largely induced as well as those classified into multiple growth and defense signaling pathways. Taken together, C₆-volatiles can serve as potential elicitors for quality formation of herbal medicines.

Introduction

Six-carbon (C₆-) volatiles, also referred to as green leaf volatiles, represent an important subset of volatile organic compounds (VOCs) derived from essential fatty acids via the hydroperoxide lyase branch of the octadecanoid pathway in plants (UL HASSAN et al., 2015). C₆-volatiles include C₆-aldehydes, alcohols, and esters such as *cis*-3-hexenal, hexanal, *trans*-2-hexenal, and *cis*-3-hexenol. They not only contribute to distinct flavors of individual foods but can serve both as defense weapons and defense signals in “green” plants. Specifically, they are not only responsible to green/beany odor that develops in damaged tissues but have emerged as key players in defense response and communications within and between plants. For example, airborne C₆-volatiles affect seedling root growth and anthocyanin accumulation in *Arabidopsis* (BATE and ROTHSTEIN, 1998) and induce volatile terpenoid production in maize (YAN and WANG, 2006). The priming effect on defense genes and metabolites has been documented in hybrid poplar (FROST et al., 2008). Their positive roles in increasing resistance to abiotic stress and fitness have been exhibited in *Arabidopsis* and *Nicotiana attenuate* (SCHUMAN et al., 2012; YAMAUCHI et al., 2015). However, these studies have seldom been carried out in medicinal plants. In order to understand their diverse roles in nature, it is necessary to explore potentially physiological and ecological functions of C₆-volatiles in medicinal plants.

Astragali Radix (AR, known as Huangqi in Chinese) is an important traditional Chinese herb and authorized as dried root of *Astragalus membranaceus* and *A. membranaceus* var. *mongholicus* in the leguminosae family. AR has been widely used as a tonic and diuretic for thousands of years. The known beneficial components contained in the herb are flavonoids, triterpene saponins and polysaccharides (SONG et al., 2014). Among these components, astragaloside IV and calycosin-7-O-β-D-glucoside are used as quality indicators of the herb and have ameliorating renal injury and immunomodulatory effects, respectively (LIU et al., 2015; SUN et al., 2016). Even though wild AR contains higher concentrations of bioactive isoflavonoids and saponins than cultivated AR (LIU et al., 2011), most commercial ARs in Chinese market are from cultivated plants due to a scarcity of the wild sources. Therefore, it is imperative to develop effective methods of improving AR quality and production for cultivated ones. In China, AR is geographically distributed in securing regions of Shanxi, Shaanxi, Gansu, Inner Mongolia, and Heilongjiang. The raw herbs grown in Hunyuan, Shanxi are well recognized as geo-authentic herbs (i.e. “Dao-di” in Chinese) because they contain relatively higher concentrations of bioactive compounds and possess a strong bean-like flavor attributed to six-carbon hexanal, hexanol and *trans*-2-hexenal (unpublished data). Chemical analysis has shown that the content of hexanal is associated with the production region and growth age of AR (SUN et al., 2010). In addition, the value of hexanal in fresh AR harvested during the traditional season was much higher than it was in ARs harvested during the other seasons (see supplemental Tab. S1). Hexanal is a dominant compound of volatile fractions contained in several herbs used in Chinese medicine, such as *Fructus Arctii*, *Herba Equiseti Hiemalis*, *Fructus Viticis*, and *Radix Bupleuri* (ZHAO et al., 2009). Thus, we hypothesize that hexanal released from aerial and belowground parts of medicinal plants plays significant roles in growth and production of bioactive compounds. The communications within and between medicinal plants mediated by soil-borne hexanal will affect the quality formation of herbal medicines.

The objective of the current study was to explore potential roles of C₆-volatiles in quality formation of herbal medicines and to understand underlying mechanism. Five-week old seedlings of *A. membranaceus* var. *mongholicus* were used as model material. The release of hexanal from the plant roots was mimicked by a below-ground exposure to synthetic hexanal for 4 weeks. The effects on seedling growth and bioactive compounds were evaluated by conventional and omics approaches at the end points of the experiment. For understanding metabolic and transcriptional changes induced by the chemical, we analyzed untargeted metabolomic and global gene expression profiles of both leaves and roots at the end points. To the best of our knowledge, this is the first study that evaluates the effects of C₆-volatiles on medicinal plants. Our findings will provide novel insights regarding the possible eco-physiological roles of C₆-volatiles playing in green plants. Additionally, our study will

* Corresponding author

shed light on potential volatile cues involved in quality formation of herbal medicine and provide potential cues that benefit to green and sustainable production of medicinal plants, especially *A. membranaceus* var. *mongholicus*

Materials and methods

Plant material and experimental design

Seeds of *A. membranaceus* var. *mongholicus* were obtained in August of 2013 from an agricultural field located in Hunyuan, Shanxi, China (1,600–1,700 m altitude, N39°34′28.66″, E113°45′31.11″) using Good Agricultural Practices. In late July of 2014, the seeds were sowed in 13-L pots (60 cm × 21 cm × 10 cm) containing a peat soil-sand mixture (Klasmann-Deilmann GmbH, Geeste, Germany). The pots were placed in an open platform at the Modern Research Center of Traditional Chinese Medicine of Shanxi University (Taiyuan, Shanxi, China) and watered when needed.

Five-week old seedlings containing four to five true leaves were used in the experiments. To mimic consecutive release of hexanal from the roots, treatment with hexanal (99%, Beijing eBio-top Technology Co. Ltd, Beijing, China) was implemented twice per week (at 2 p.m. on Tuesdays and Fridays) for four weeks. There were four groups in this experiment: control (without any treatment), 10 μM hexanal, 50 μM hexanal, and 100 μM hexanal, which are less than 1% of the content of hexanal contained in 10 g of 2-year old plant roots (diameter: 0.4–1.0 cm; height: 10 cm) at the vegetative season, flowering season and traditional harvest season during a phenological period. The details on the quantification of hexanal were presented in supplemental file and the content of hexanal was listed in supporting Tab. S1.

A total of 30 seedlings, which included two biological replicates (n=15), were used in each group. The absolute mass of hexanal was calculated based on the volume of the cultivation matrix in each pot and the concentration of hexanal applied. Briefly, sterile cotton balls embedded in pure hexanal were placed in Eppendorf tubes with artificial holes. The tubes were immediately placed into the culture matrix using sterile forceps at five equidistant points. In each application, fresh chemical, cotton balls, and tubes were used and the old ones were removed. At the end of the experiment, roots and true leaves (2nd and 3rd) were harvested from at least nine seedlings per replicate and stored at -20 °C for chemical analyses and chlorophyll quantification. Seedling height, true leaf number, and root diameter as well as mass of below- and above-ground parts were recorded at the beginning and the end of the experiment. For global gene expression profile analysis, leaf and root specimens were collected on ice and stored at -70 °C after immediately freezing in liquid nitrogen.

Quantification of polysaccharides in roots and of chlorophyll a/b in leaves

For polysaccharide quantification, each root specimen was first ground into a fine powder in liquid nitrogen and divided into two parts. One part was oven-dried at 105 °C for 12 h and used for the determination of water content. The second part was weighed and refluxed three times with 20 volumes of distilled water for 1 h. The extract was filtered while hot, and the filtrate was evaporated under vacuum to approximately 5 mL. Absolute ethanol was added to achieve an ethanol concentration of approximately 80%. The solution was kept at 4 °C for 24 h and concentrated under vacuum. The concentrates were washed twice with 70% ethanol and dissolved in distilled water. Following the removal of insoluble compounds by centrifugation (2,000 g for 5 min at 4 °C), the volume of the solution was adjusted to 2 mL. The quantification was performed by the method described elsewhere (SUN et al., 2010).

For chlorophyll quantification, 0.1 g leaf tissue was ground into a

fine powder and extracted with 10 mL of absolute ethanol:acetone (1:1, v:v) in the dark until the powder was white. The extract was centrifuged at 10,000 g for 5 min at 4 °C, and the resulting supernatant was spectrophotometrically analyzed at 645 and 663 nm (Cary 50 Spectrophotometer, Agilent, Santa Clara, USA). The contents of chlorophyll a and chlorophyll b were measured by the method described by ARNON (1949).

Root and leaf metabolomic profiles

Metabolomic profiles were obtained by ultra-performance liquid chromatography (UPLC)-quadrupole time-of-flight (QTOF)-mass spectra (MS). Briefly, 200 mg of fresh specimens were ground into a fine powder and extracted with 20 volumes of 70% ethanol (chromatographic grade, v/v) and acetic ether (chromatographic grade) in an ultrasonic bath for 30 min, respectively. Filtrates were pooled, concentrated, and dissolved in ethanol of chromatographic grade. Finally, the volume of the solution was adjusted to 2 mL. Ethanol and acetic ether of chromatographic grade were bought from Tianjin Guangfu Fine Chemical Research Institute (Tianjin, China).

Extracts (1 μL) were injected into a Waters Acquity UPLC I Class system (Waters Corporation, Milford, MA, USA) coupled to a PDA detector and a high-resolution Waters Zevo-G2-S Q-TOF mass spectrometer (Waters Corporation, Manchester, UK). Electrospray ionization in positive and negative modes was used to ionize compounds separated by an Acquity HSS T3 column (100 × 2.1 mm, 1.8 μm). Water and solvents used in the extraction were included as controls to assess the contribution of the separation process and extraction methods to the overall signals. Additional mixed samples prepared from each group were used as quality control and injected once every 12 samples.

Chromatography was performed at 0.5 mL/min (flow rate) and 40 °C (column temperature). The mobile phases A and B consisted of 0.1% formic acid and acetonitrile with 0.1% formic acid, respectively. The gradient elution was programmed as follows, 0–0.3 min, 95% A; 0.3–0.8 min, 95%→82% A; 0.8–5.0 min, 82%→60% A; 5.0–7.5 min, 60%→20%; 7.5–9.0 min, 20% A; 9.0–10.0 min, 20%→2% A; 10.0–12.0 min, 2% A; and 12.0–12.3 min, 2%→95% A.

The mass spectra conditions consisted of a drying gas (N₂) flow rate of 15 L/min, a desolvation temperature of 450 °C, a capillary voltage of 500 V for ESI (+) and 2,000 V for ESI (-), a collision energy of 45–60 V, a cone voltage of 40 V, and an ion source temperature of 100 °C. The collision energy was set at 6 eV (trap) for low-energy scan, 50–70 eV ramp for ESI (-), and 45–60 eV ramp for ESI (+) in high-energy scan. The full scan data acquisition range was between 50 and 1,500 Da. Mass accuracy was maintained using a lock spray with leucine enkephalin (Cat no. 700002456, Waters Corporation, USA) at a concentration of 200 pg/μL and a flow rate of 10 μL/min (m/z 556.2766 ESI [+] and 554.2620 ESI [-]). The instrument was controlled by Masslynx 4.1 software (Waters Corporation).

All MS data were processed with UNIFI 1.7.1 (Waters Corporation, USA). Data within UNIFI 1.7.1 were subjected to apex peak detection and alignment processing algorithms, which enables related ion compounds to be grouped together and analyzed as a single entity.

Processing of metabolomic data

Raw data were processed and normalized in an untargeted manner by extracting and aligning all mass signals with a signal-to-noise ratio of at least 3 using Progenesis QI (Waters Corporation). This resulted in a data matrix of 8,291 mass signals × 48 samples. The noise level in the data was 23% (< 50%), indicating that the variation in the dataset was effective for analysis. Identification of bioactive metabolites was based on the mass sizes of quasi-molecules and representative fragment ions. Additionally, online XCMS (version 2.0.1,

https://xcmsonline.scripps.edu/), an evolved cloud-based platform for metabolomics and mass spectrometry, was used to evaluate dysregulated intermediate and terminal metabolites (BENTON et al., 2015).

RNA extraction, next generation transcriptome sequencing, and sequencing assembly

Fresh leaves and roots from two biological replicates of the control and the treatment with 50 μM hexanal were ground respectively to a fine powder in liquid nitrogen. Total RNA was extracted using RNAiso Plus (Code No. 9109, Takara, Dalian, China) according to the manufacturer's instruction. To eliminate genomic DNA, total RNA was treated with RNase-free DNase I (Code No. 2270A, Takara) and monitored on 1% agarose gels for primary quality evaluation. Following a primary check of the purity by NanoPhotometer[®] spectrophotometer (Implen, CA, USA), accurate concentration of total RNA was measured using Qubit[®] RNA Assay Kit in Qubit[®] 2.0 Fluorometer (Life Technologies, CA, USA). Lastly, RNA integrity was assessed using the RNA Nano 6000 Assay Kit of the Agilent Bioanalyzer 2100 system (Agilent Technologies, CA, USA) for constructing RNA-seq library purpose.

For constructing transcriptome library, 3 μg of pooled RNA equally from root and leaf tissues was used as input material for RNA sample preparations for economic reason. Sequencing libraries were generated using NEBNext[®] Ultra[™] RNA Library Prep Kit for Illumina[®] (NEB, USA) following manufacturer's recommendations, which was then subjected to transcriptome sequencing with the HiSeq 2500 platform (Illumina, San Diego, Ca, USA) to produce 125 bp single end reads. Adapter sequences were trimmed off using the cutadapt program (MARTIN, 2011). Sequence reads were assembled with Trinity (Version: trinityrnaseq_r2013-02-25) in Chrysalis clusters mode. Resulting Unigenes annotated with BlastX against public databases including NR, NT, CDD, PFKM, Swittport, TrEMBL, GO and KEGG. Expression levels were calculated using the RSEM software package and marked as PFKM values (LI and DEWEY, 2011).

Statistical analysis

The impact of different concentrations of hexanal on plant growth and bioactive compounds was evaluated using one-way analysis of

variance (ANOVA) with the software of GraphPad Prism 5.01 (California, USA). All comparisons of the mentioned parameters including secondary metabolites identified by UPLC-Q-TOF MS were calculated using Tukey-tests at a significance level of $P < 0.05$. Mean values labeled with different letters indicate significant differences. The mean variability is shown as standard deviation. To identify functional genes induced by hexanal, a hypergeometric test (phyper), a widely used algorithm, was performed to calculate the P -values of GO and pathway terms (AUDIC and CLAVERIE, 1997). Then P -value was calibrated with FDR. Those with FDR value ≤ 0.001 and fold change ≥ 2 denote significant differences.

Results

Effect of hexanal on seedling growth and photosynthetic parameters

Although root and shoot length, root diameter, number of mature leaves, fresh weight of below- and above-ground parts were measured, the analysis revealed that below-ground hexanal treatment had no significant effects on root growth but had negative effects on aerial growth (Fig. 1). Specifically, 10 and 100 μM hexanal resulted in significant decrease in the shoot length but 50 μM hexanal kept the growth rate at the same level as it was in the control.

Effect of hexanal on leaf photosynthesis was evaluated by chlorophyll a and chlorophyll b contents as well as the ratio of chlorophyll a to chlorophyll b. The result was also presented in Fig. 1. Compared to the control, all hexanal treatments decreased leaf chlorophyll a and b contents. In addition, 100 μM hexanal obviously decreased the ratio of chlorophyll a to chlorophyll b.

Effect of hexanal on root polysaccharide accumulation

Because a significant correlation between the contents of hexanal and polysaccharides contained in the raw herb has been detected in a previous study (SUN et al., 2010), effect of hexanal on root polysaccharide accumulation was examined (see Fig. 2). Following a four-week treatment with 50 μM hexanal, polysaccharide concentration significantly increased in seedling roots. On the other hand, 10 μM and 100 μM hexanal had no significant effects on root polysaccharide accumulation since there was no obvious difference in the con-

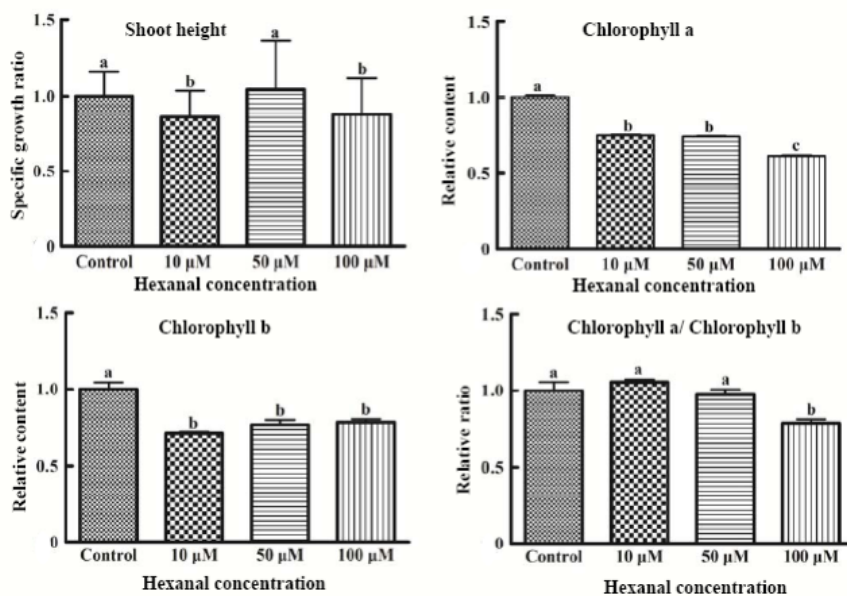


Fig. 1: Effect of hexanal on *A. membranaceus* var. *mongholicus* growth and photosynthesis.

Data are normalized values to the values obtained in the control group. Means (\pm standard deviation) followed by the same letter are not significantly different according to one-way ANOVA ($P < 0.05$).

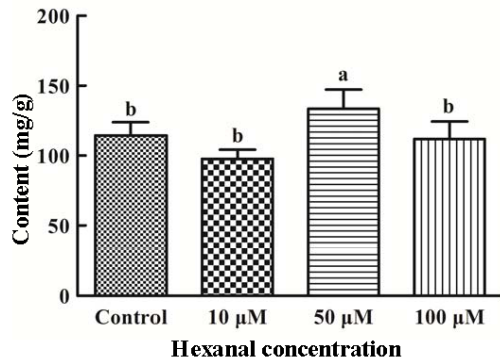


Fig. 2: Effect of hexanal on polysaccharide accumulation in roots. Different letters above the bar indicates the significant difference in the concentration.

centration of polysaccharides between the control and the treatments of 10 μ M and 100 μ M hexanal.

Effect of hexanal on secondary metabolites in roots/leaves

Flavonoid and saponin compounds constituent most of secondary metabolites identified in *A. membranaceus* var. *mongholicus* (LIU et al., 2011). Up to now, approximately 30 flavonoids and 40 saponins have been isolated and identified from the plant species. Based on mass and mass spectra, 18 flavonoids and 11 saponins including two isomers were identified. Detail information on the compounds was listed in supplemental Tab. S2.

Using normalized intensity data, we examined the effect of hexanal on their accumulations in seedling roots and leaves. The results revealed that hexanal treatment had no significant effects on their accumulations in leaves, with the exception of malonylastragaloside I, the accumulation of which was reduced in the group of 50 μ M hexanal (Tab. 1). On the other hand, hexanal treatment significantly affected the accumulation of root metabolites, with the exception

of the follows: isoquercitroside, isoliquiritigenin, ononin, calycosin-7-O- β -D-glucoside, isomucronulatol 7-O- β -D-glucoside, Huangqi-yenin D, 9,10-dimethoxypterocarpan-7-O- β -D-glucopyranoside, 2R-farrerol-7-O- β -D-glucoside, and (3R)-8,2'-dihydroxy-7,4-dimethoxy-isoflavon.

The flavonoid compounds that were obviously affected by hexanal treatment were demonstrated in Tab. 1, accounting for 50% of flavonoid compounds identified. Briefly, hexanal treatments increased the contents of pratensein-7-O- β -D-glucoside, malonylrhamnocitrin-3-O- β -D-glucoside, formononetin-7-O- β -D-glc-6''-O-malonate, and astragalin in roots. And this improving effect displayed clear dose dependence. Meanwhile, the concentrations of formononetin and calycosin in all treatments were at the same level to that they were in the control, but the values in 50 μ M hexanal treatment were significantly higher than the other treatments. Additionally, isorhamnetin-3-O- β -D-glucoside level in seedling roots was significantly reduced in all treatments while the reduction of (6aR, 11aR)-3, 9, 10-trinethoxypterocarpan level was dependent on the concentration of hexanal applied.

The intermittent exposure to hexanal increased the contents of all saponin compounds identified excluding cyclocanthoside E in seedling roots (Tab. 1). Compared to the control, 50 μ M and 100 μ M hexanal effectively increased the accumulations of mongholicoside I, methylastragaloside II, astragaloside II, isoastragaloside II, and isoastragaloside IV. In addition, 50 μ M hexanal significantly increased soyasaponin I concentration while the other treatments had no obvious effect. Meanwhile, a significantly increased accumulation of mongholicoside II was only detected in 100 μ M hexanal treatment.

Effects of hexanal on leaf and root metabolite profiles

Relative to 10 and 100 μ M hexanal, 50 μ M hexanal was more effective in increasing the root concentrations of bioactive compounds (i.e., polysaccharides, flavonoids, and saponins) as described above. At the same time, 50 μ M hexanal had a slight inhibitory effect on shoot growth (i.e., shoot height, true leaf number, and photosynthetic

Tab. 1: Effect of hexanal on accumulations of flavonoid and saponin compounds in seedling roots/leaves

Secondary metabolites	Control	10 μ M	50 μ M	100 μ M
(6aR,11aR)-3,9,10-trinethoxypterocarpan	1.00 \pm 0.06 ^b	1.38 \pm 0.07 ^a	0.62 \pm 0.03 ^c	0.34 \pm 0.01 ^d
Isomucronulatol- 7-O- β -D-glucoside	1.00 \pm 0.01 ^a	1.12 \pm 0.02 ^a	1.10 \pm 0.01 ^a	0.40 \pm 0.03 ^b
Pratensein-7-O- β -D-glucoside	1.00 \pm 0.02 ^b	1.31 \pm 0.06 ^a	1.37 \pm 0.08 ^a	1.32 \pm 0.03 ^a
Calycosin	1.00 \pm 0.01 ^{ab}	0.87 \pm 0.11 ^{ab}	1.18 \pm 0.10 ^a	0.74 \pm 0.05 ^b
Astragalin (Kaempferol 3-O- β -D-glucoside)	1.00 \pm 0.05 ^c	1.22 \pm 0.12 ^{bc}	1.71 \pm 0.06 ^a	1.60 \pm 0.15 ^{ab}
Isorhamnetin-3-O- β -D-glucoside	1.00 \pm 0.07 ^a	0.50 \pm 0.01 ^c	0.72 \pm 0.06 ^b	0.48 \pm 0.01 ^c
Malonylrhamnocitrin-3-O- β -D-glucoside	1.00 \pm 0.04 ^b	1.21 \pm 0.07 ^{ab}	1.26 \pm 0.06 ^a	1.31 \pm 0.05 ^a
Formononetin	1.00 \pm 0.10 ^{ab}	0.70 \pm 0.10 ^b	1.14 \pm 0.09 ^a	0.68 \pm 0.05 ^b
Formononetin-7-O- β -D-Glu-6''-O-malonate	1.00 \pm 0.22 ^b	1.42 \pm 0.25 ^b	1.65 \pm 0.29 ^{ab}	2.5 \pm 0.08 ^a
Mongholicoside I	1.00 \pm 0.12 ^b	1.20 \pm 0.11 ^{ab}	1.37 \pm 0.07 ^a	1.41 \pm 0.04 ^a
Isoastragaloside IV	1.00 \pm 0.17 ^b	1.37 \pm 0.18 ^b	2.04 \pm 0.18 ^a	2.20 \pm 0.02 ^a
Astragaloside IV	1.00 \pm 0.05 ^b	1.15 \pm 0.07 ^{ab}	1.17 \pm 0.04 ^{ab}	1.22 \pm 0.03 ^a
Astragaloside II	1.00 \pm 0.09 ^c	1.15 \pm 0.11 ^{bc}	1.59 \pm 0.12 ^{ab}	1.79 \pm 0.12 ^a
Isoastragaloside II	1.00 \pm 0.04 ^b	0.76 \pm 0.15 ^b	1.79 \pm 0.06 ^a	1.51 \pm 0.17 ^a
Methylastragaloside II	1.00 \pm 0.32 ^b	3.14 \pm 0.49 ^a	3.55 \pm 0.38 ^a	3.37 \pm 0.15 ^a
Soyasaponin I	1.00 \pm 0.42 ^b	1.31 \pm 0.82 ^b	4.42 \pm 0.70 ^a	1.71 \pm 0.58 ^b
Malonylastragaloside I*	1.00 \pm 0.12 ^a	0.83 \pm 0.12 ^a	0.39 \pm 0.07 ^b	0.68 \pm 0.12 ^{ab}
Cyclocanthoside E	1.00 \pm 0.07 ^a	0.22 \pm 0.06 ^b	0.39 \pm 0.07 ^b	0.35 \pm 0.03 ^b
Mongholicoside II	1.00 \pm 0.10 ^b	1.19 \pm 0.06 ^{ab}	1.24 \pm 0.04 ^{ab}	1.26 \pm 0.03 ^a

Data are expressed in relative values normalized to the values obtained in the control group. Mean values (\pm standard error) labeled with the same superscript letter indicate no significant difference according to Tukey-test ($p < 0.05$). The compound marked with star was measured in leaves.

parameters). Therefore, 50 μM hexanal exhibited a better balancing effect on *A. membranaceus* var. *mongholicus* seedling growth and accumulations of bioactive compounds. To identify all possible metabolic intermediates and end products, raw datasets obtained from the control and 50 μM hexanal groups were uploaded and analyzed using online XCMS platform.

Pairwise analyses demonstrated that there were 473 features (i.e., identified or unidentified metabolites based on the mass-to-charge ratio (m/z) and retention time; P value ≤ 0.01 and fold change ≥ 1.5) in positive mode and 413 features in negative mode in leaves. Additionally, 51 and 50 dysregulated features were obtained in roots in positive and negative modes, respectively. That was to say, the leaves had more dysregulated features than the roots following exposure to hexanal (Fig. 3).

Identification of the dysregulated features revealed that a big part was derived from metabolisms of glycerophospholipids and triacylglycerols (See supplemental Tab. S3). Specifically, the application of 50 μM hexanal resulted in increase in the levels of (13*S*)-hydroxyoctadecadienoic acid (13[S]-HPOD), (10*E*,12*Z*,15*Z*)-(9*S*)-9-hydroperoxyoctadeca-10,12,15-trienoic acid (9[S]-HPOT), (10*E*,12*Z*)-(9*S*)-9-hydroperoxyoctadeca-10,12-dienoic acid (9[S]-HPOD), (9*Z*,11*E*)-13-oxooctadeca-9,11-dienoic acid (13-KODE), stearidonic acid, and linolenic acid in seedling roots. In addition, the leaf concentrations of coenzyme A (CoA) compounds (i.e., acetyl-CoA, [S]-3-hydroxyhexanoyl-CoA, 3-oxo-cis-8-tetradecenoyl-CoA, decanoyl-CoA, and 6-dodecenoyl-CoA) derived from lipid oxidation increased upon treatment. Corresponding mass spectra are listed in supporting Tab. S4.

Effect of hexanal on leaf and root gene expression profiles

In order to monitor transcriptional changes in seedling leaves and roots upon treatment, global gene expression profiles were compared between the control and 50 μM hexanal groups. Totally, 82,619 Unigenes (designed as All-Unigenes) were obtained from the two transcriptome libraries. The total length for All-Unigenes was 90,944,019 nt, meaning that the average length was 1101 nt for each Unigene. For functional annotation, 56,747, 58,357, 37,079, 33,800, 21,904, and 44,178 All-Unigenes were annotated to the NR, NT, Swiss-Prot, KEGG, COG, GO databases, respectively, accounting for 75.72 percent of the total amount of All-Unigenes. The distributions of e -value, similarity, and species resulting from NR annotation were demonstrated in Fig. 4. It showed that more than 80% of All-Unigenes were distributed in the Legume family (i.e. *Glycine max*, *Medicago truncatula*, and *Locus corniculatus* var. *japonicus*), suggesting that the resulting dataset was competent and could be used to test gene expression changes induced by hexanal. To understand the distribution of gene function, GO classification for All-Unigenes was further performed by WEGO software after GO function was annotated via Blast2GO program using the dataset from NR annotations. The result was presented in supplemental Fig. S1.

For individual library, 81,297 Unigenes averaging 883 bp in the length were obtained in the control while 86,129 Unigenes averaging 900 bp obtained in the treatment, covering 78.92% and 85.23% of the total length of All-Unigenes. Significant test further showed that the treatment resulted in 5,791 differentially expressed genes (DEGs) (2-fold or greater; false discovery rate (FDR) ≤ 0.001). Corresponding scatter patterns of DEGs were presented in Fig. 5. Among DEGs,

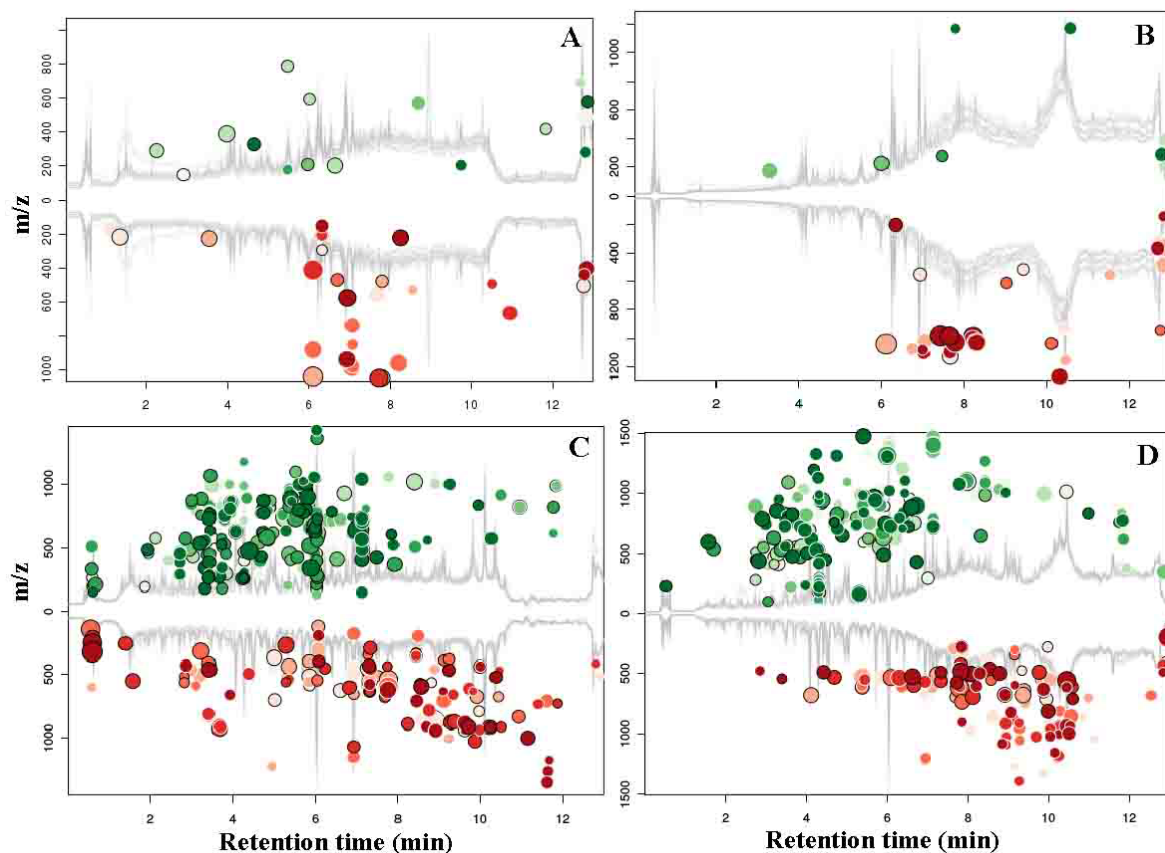


Fig. 3: Differential metabolite plots (cloud plots) obtained from root (A, B) and leaf (C, D) metabolomic datasets of the 50 μM hexanal treatment and control. A and C correspond to the datasets obtained in the positive mode, while B and D correspond to the datasets obtained in the negative mode. Only metabolites that were dysregulated ($P \leq 0.01$; fold change ≥ 1.5) are presented. Up-regulated metabolites are shown in green; down-regulated metabolites are shown in red. The size of each circle corresponds to the log-fold change of the feature. The shade of the bubble corresponds to the magnitude of the P -value (the darker the color, the smaller the P -value).

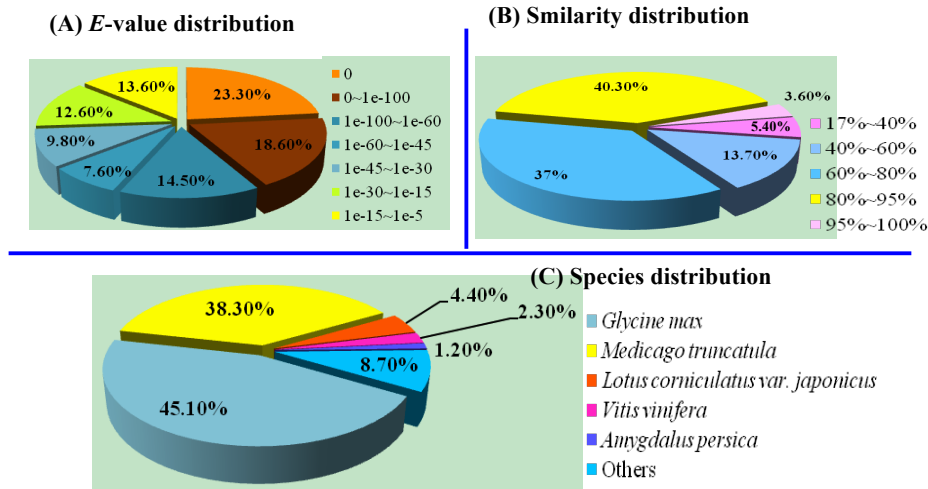


Fig. 4: Distribution of *e*-value (A), similarity (B), and species (C) resulting from NR annotations for All-Unigenes.

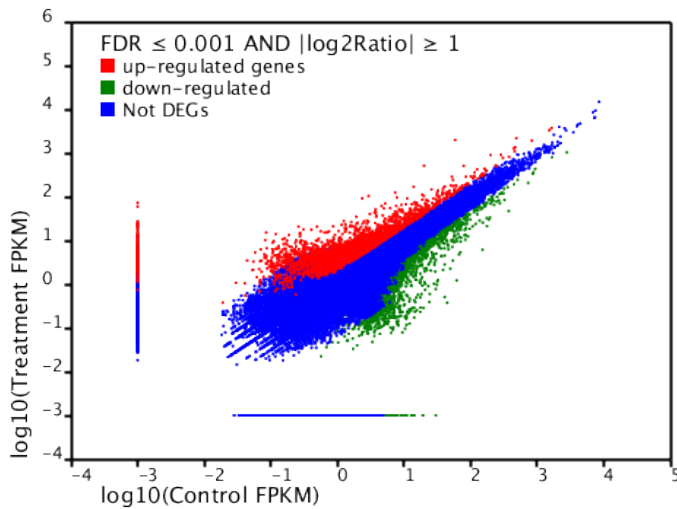


Fig. 5: Scatter diagram of differentially expressed genes (DEGs) when compared to the control.

In the diagram, the genes were classified in three classes. Red genes are up-regulated while green ones are down-regulated. Blue ones are not differentially expressed genes. The horizontal coordinates indicate the expression level of the control and the vertical coordinates mark the expression level of the treatment.

317 were only expressed in the control while 387 were expressed upon the treatment. For these co-expressed in both the control and treatment, 2,556 genes were down-regulated and 2,531 up-regulated. When compared to annotation pattern resulted from All-Unigene dataset, a few differences in the percentage of DEGs falling into specific ontology groups were observed. This holds especially for those assigned to the categories of biological process and molecular function (Fig. 6). In particular, the proportion of DEGs annotated as following: biological adhesion, rhythmic process, channel regulatory activity, metallochaperone activity, molecular transducer activity, protein tag, receptor activity, and structural molecular activity was reduced upon the treatment. Meanwhile, the proportion of DEGs annotated as immune system process, locomotion, antioxidant activity, electron carrier activity, nutrient reservoir activity, and translation regulator activity was increased.

Totally, 2,518 DGEs were annotated into 125 pathways. And the number of DEGs annotated as metabolic pathways (675) and biosynthesis of secondary metabolites (408) was highest, followed by the

pathways annotated as “plant-pathogen interaction” (217) and “plant hormone signal transduction” (175). In addition, there was a large part of DEGs associated with metabolisms of lipid, carbohydrates, terpenoids, polyketides and other secondary metabolites. The detail information on pathway enrichment was presented in Tab. 2.

In response to jasmonate signaling, temporal dynamics of growth and photosynthesis suppression occurred, providing evidence that defense signaling interacted with growth signaling (ATTARAN et al., 2014). As described above, the treatment with soil-borne hexanal affected the seedling growth and secondary metabolism and seedling leaves contained more dysregulated metabolites than roots upon treatment. It means that signal exchange between below- to above-ground parts occurred. In order to find out potential genes involved in growth signaling and defense signaling, we mapped the signaling pathways using DEGs annotated as “plant hormone signal transduction”. The map was presented in Fig. 7. It demonstrated that hormone crosstalk induced by hexanal was extensive and involved in follow hormones: salicylic acid (SA), abscisic acid (ABA), auxin, cytokinine, gibberellins (GA), brassinosteroid acid, ethylene (ET) and jasmonic acid (JA). Bi-directional regulation was observed for all of the signaling pathways involved, especially for key transcription factors in each signaling pathway.

Discussion

Bioactivities of C₆-volatiles are associated with the volatile saturation

Upon mechanical wounding, herbivore attack, or abiotic stresses, C₆-volatiles are formed rapidly, within seconds or minutes. Thus, they constitute essential components of plant defense system. At the beginning, their ecological and physiological functions have been investigated, especially the effect on insect herbivores and pathogens. A combination of hexanal and hexanol enhanced insect pheromone response while *trans*-2-hexenal and *cis*-3-hexenal were inactive (DICKENS, 1990). When exposed to saturating vapors of C₆-aldehydes, seed germination of soybean, *Glycine max*, was inhibited in the order: *trans*-2-nonenal > *trans*-2-hexenal > hexanal (GARDNER et al., 1990). Relative to *trans*-2-hexenal, hexanal exhibited a reduced inhibitory effect on fungal growth and aflatoxin production (CLEVELAND et al., 2009). In *Arabidopsis*, the same concentrations of hexanal, *trans*-2-hexenal and *cis*-3-hexenal up-regulated *lipoxygenase* (*LOX*) to different degrees, the induction of hexanal was inferior to the others (BATE and ROTHSTEIN, 1998). In developing cotton bolls, *trans*-2-hexenal induced the formation of scopoletin, 2,7-dihydroxycadalene, lacinilene C and methyl ester but hexanal had no

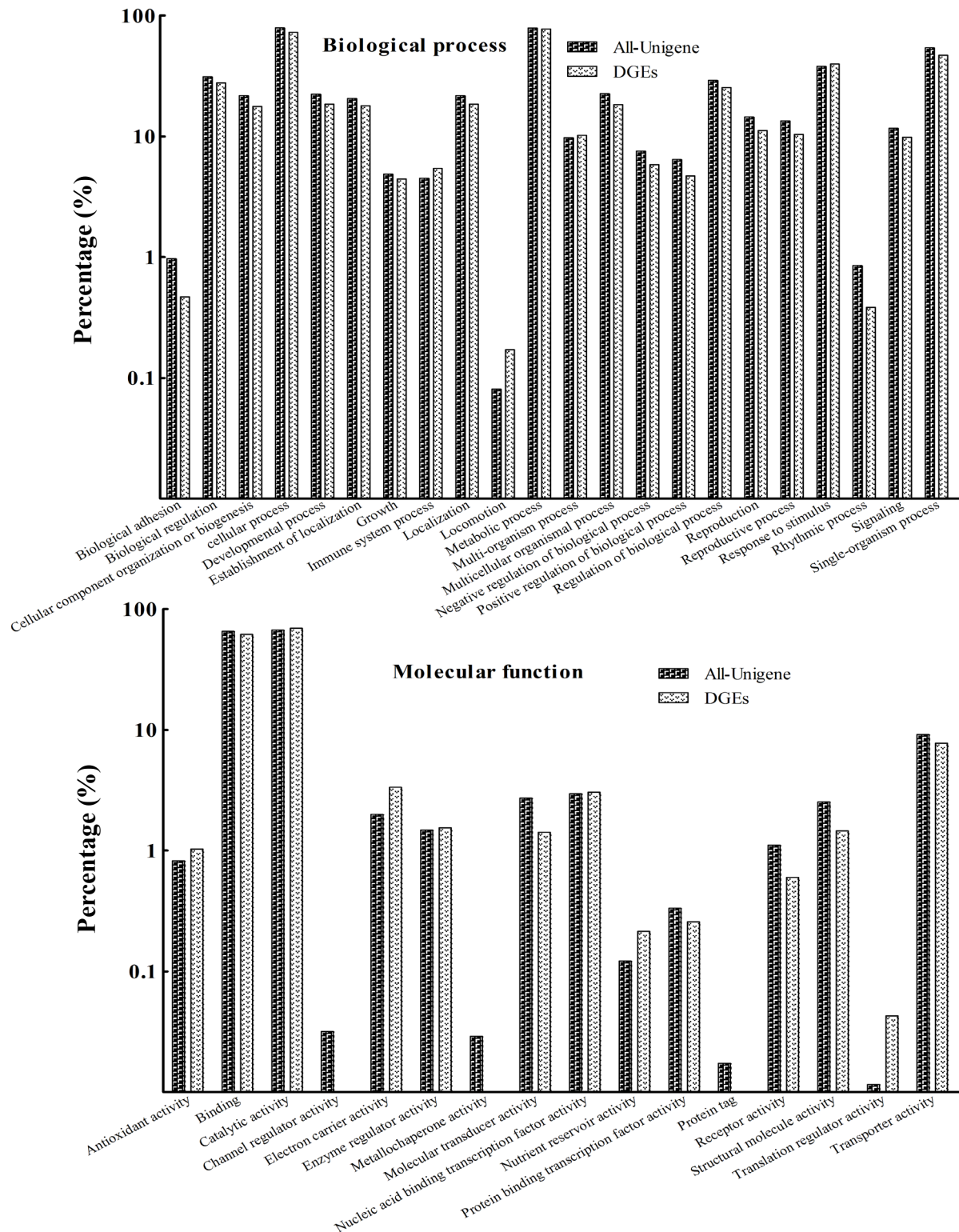


Fig. 6: Percentages of DEGs and All-Unigenes annotated as GO terms within the categories of biological processes and molecular function.

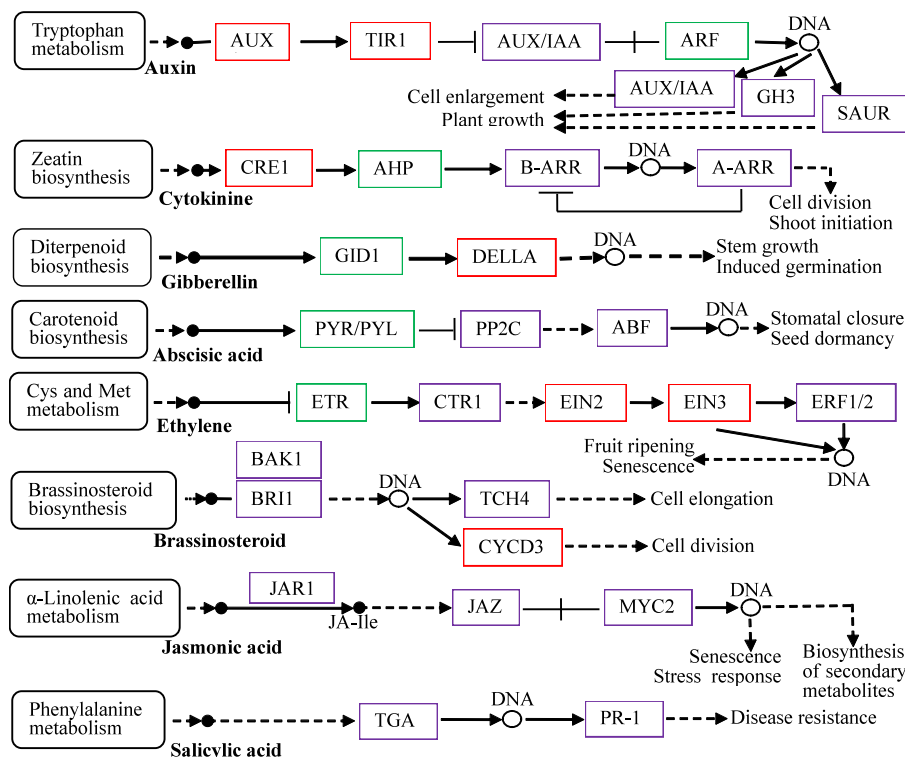
effect (ZERINGUE, 1992). In rough lemon, *trans*-2-hexenal induced expression of *RlemLOX*, *RlemHPL* and allene oxide synthase (AOS) gene but hexanal suppressed their expression (GOMI et al., 2003). By monitoring expression profiles of the genes involved in defense responses in *Arabidopsis*, it was conferred that induction of unsaturated C₆-volatiles was associated with the volatile used (KISHIMOTO et al., 2005). In *A. membranaceus* var. *mongholicus* seedlings,

4-week intermittent exposure to hexanal resulted in an inhibitory effect on shoot growth but promoted accumulation of bioactive compounds in roots, coinciding with global changes in metabolite and gene expression profiles. As hexanal and hexanol are saturated and *trans*-2-hexenal and *cis*-3-hexenal are unsaturated, distinct difference in physiological roles of C₆-volatiles in plants should be related to the volatile saturation.

Tab. 2: Top pathways resulting from KEGG enrichment of DEGs.

Level 3	DEGs	ID	Level 2
Biosynthesis of secondary metabolites	408	Ko01110	Global map
Plant-pathogen interaction	217	Ko04626	Environmental adaptation
Plant hormone signal transduction	175	Ko04075	Signal transduction
Starch and sucrose metabolism	102	Ko00500	Carbohydrate metabolism
Glycerophospholipid metabolism	96	Ko00564	Lipid metabolism
Ether lipid metabolism	70	Ko00565	
Linoleic acid metabolism	20	Ko00591	
Cutin, suberine and wax biosynthesis	26	Ko00073	
alpha-Linolenic acid metabolism	31	Ko00592	
Fatty acid metabolism	27	Ko00071	
Zeatin biosynthesis	80	Ko00908	Metabolism of terpenoids and polyketides
Terpenoid backbone biosynthesis	57	Ko00900	
Limonene and pinene degradation	31	Ko00903	
Carotenoid biosynthesis	27	Ko00906	
Phenylpropanoid biosynthesis	77	Ko00940	Biosynthesis of other secondary metabolites
Flavone and flavonol biosynthesis	46	Ko00944	
Stilbenoid, diarylheptanoid and gingerol biosynthesis	47	Ko00945	
Flavonoid biosynthesis	42	Ko00941	

KEGG Pathway is divided in three levels and level 3 owns the detailed pathway graph and response gene. Here, 2,518 differentially expressed Unigenes (DEGs) were annotated to each level in a 3 pathway graph through mapping. Detail information of level 3 were listed (i.e. GO terms, the number annotated in DEGs, Pathway ID and corresponding level 2).

**Fig. 7:** Signal transduction pathways induced by hexanal.

The red block indicates up-regulation of the DEGs while the green one indicates down-regulation. And the box marked with combined red and green means that the expression was regulated bi-directionally.

Effect of C₆-volatiles on plant growth and secondary metabolism is dose-dependent

In *Arabidopsis*, the aerial treatment with 10 μ M *trans*-2-hexenal had a moderate effect on growth while 100 μ M of *trans*-2-hexenal severely affected root morphology and moderately affected shoot development (BATE and ROTHSTEIN, 1998). In soybean plant, 0.9 μ g

of hexenal/mL of air delivered via a flow-through system (100 mL/min) inhibited seed germination by 50% and 1.8 μ g of hexenal/mL of air inhibited 100% of seed germination (GARDNER et al., 1990). Dose-dependent priming effect of *trans*-2-hexenal on anthocyanin accumulation was observed in *Arabidopsis* upon treatment with MeJA (HIRAO et al., 2012). In specific, pretreatment with 50 nmol

trans-2-hexenal resulted in highest content while pretreatment with 25 and 100 nmol had comparable contents. In *A. membranaceus* var. *mongholicus*, 50 μ M hexanal exhibited a slight inhibitory effect on shoot growth but significantly enhanced accumulations of bioactive compounds (e.g. polysaccharides, astragaloside II, isostragaloside II and methylastragaloside II) in roots. Taken together, effects of C₆-volatiles on plant growth and secondary metabolites are dose-dependent. Therefore, it is vital to screen suitable doses of C₆-volatiles when applied in plants of economic or medical importance.

Up-regulation of lipid metabolism induced by hexanal

13/9[S]-HPOD, 13-KODE and 9[S]-HPOT are intermittent products derived from polyunsaturated fatty acids (PUFAs) and can be transformed into C₆-volatiles or JA signal through the action of LOX, AOS and HPL in plants. Stearidonic acid and linolenic acid belong to PUFAs and can be released from membrane lipids upon biotic and abiotic stresses (WASTERNAK and HAUSE, 2013). Therefore, increased levels of PUFAs and their hyperoxides in *A. membranaceus* var. *mongholicus* roots might be related to the up-regulation of JA signaling pathway or production of C₆-volatiles. Acetyl-CoA and malonyl-CoA are the first substrates in the biosynthetic pathways of flavonoids and terpenoids, respectively (PAN et al., 2007; MOSES et al., 2014). Upon treatment with hexanal, CoA compounds in leaves increased coinciding with enhanced contents of polysaccharides and secondary metabolites in roots, it is reasonable to deduce that below-ground hexanal promoted the accumulations of bioactive compounds in roots by up-regulating lipid oxidation in *A. membranaceus* var. *mongholicus*. Therefore, lipid metabolism should be involved in the induction of hexanal in *A. membranaceus* var. *mongholicus*. Further studies should be carried out to understand the role of lipid metabolites in the induction of hexanal, especially their roles in the biosynthesis of polysaccharides, flavonoids and saponins.

Multiple signaling pathways and source-sink dynamic should be involved in the induction of hexanal

Using *Arabidopsis* mutants deficient in the signaling pathways, it was suggested that ET-, JA-, and phytoalexin (PAD2)-dependent signaling pathways were simultaneously activated by C₆-aldehyde treatment (KISHIMOTO et al., 2006). Octadecanoid signaling pathway was involved in the induction of *cis*-3-hexenyl acetate (ζ 3HAC) in *Zea mays* (ENGELBERTH et al., 2007). Higher concentrations of JA and linolenic acid were detected in ζ 3HAC-exposed leaves of hybrid poplar following gypsy moth feeding (FROST et al., 2008). By microarray method, significant expression of genes involved in transcriptional regulation, Ca²⁺- and lipid signaling, and cell wall reinforcement was induced by *cis*-3-hexenol (ENGELBERTH et al., 2013). In MeJA-treated *Arabidopsis* plants, chlorophyll concentrations decrease and surface anthocyanin concentrations increase (JUNG, 2004). In rice, the expression of genes involved starch synthesis is regulated by ET and ABA signaling (ZHU et al., 2011). Along with increased hyperoxidation of PUFAs, the below-ground exposure to hexanal enhanced accumulations of polysaccharides and secondary metabolites in *A. membranaceus* var. *mongholicus* roots and decreased chlorophyll contents in leaves, suggesting that the induction of hexanal was involved in ET, JA, and ABA signaling pathways. Consistently, transcription of genes annotated as “plant hormone signal transduction”, “biosynthesis of secondary metabolites”, “lipid metabolism”, “starch and sucrose metabolism” was enhanced. On the other hand, the proportion of gene transcripts annotated as “locomotion” and “nutrient reservoir activity” was increased coinciding with higher dys-regulated features in leaves. Thus, signal exchange and source-sink dynamic between above- and below-ground parts should

be occurred upon treatment with hexanal. In order to understand underlying mechanism, spatiotemporal patterns of signaling pathways and biosynthesis of secondary metabolites should be performed.

Conclusion and recommendation

Six-carbon volatiles are an important subset of volatile organic compounds contributing to distinct flavors possessed by herbal medicines. Meanwhile C₆-volatiles can serve as defense weapons and defense signals simultaneously. By mimicking the consecutive release of hexanal from *A. membranaceus* var. *mongholicus* roots, our study has shown that hexanal plays role on growth and bioactive compounds of medicinal plants in a dose-dependent pattern. A moderate concentration of hexanal has no negative effect on seedling growth but significantly promotes the accumulations of polysaccharides, flavonoid and saponin compounds in roots. Traditionally, the content of hexanal is associated with the production region, growth age, harvest season and planting pattern of the herbs. Thus our work provides evidence that the release of C₆-volatiles from medicinal plants might influence the production and quality of herbal medicine, especially the accumulations of bioactive polysaccharides and non-volatile secondary products. Hence, our study should provide alternative chemical cues for quality improvement of herbal medicines when cultivated in the fields. Our work will benefit to the development of eco-friendly technologies for sustainable production of *A. membranaceus* var. *mongholicus* for medical purpose.

Acknowledgements

This work was supported by the Shanxi Scholarship Council of China (grant number 2013-021), the Natural Science Foundation of Shanxi Province (grant number 2014011047-3), the 48th Scientific Research Foundation for the Returned Overseas Chinese Scholars of State Education Ministry and the Postdoctoral Science Foundation of China (grant number 2014M560170), and the Collaborative Innovation Center of Astragali Radix Resource Industrialization and Internationalization (grant number HQTCXZX2016-003).

References

- ARNON, D.I., 1949: Copper enzyme in isolated chloroplasts. Polyphenoloxidase in *Beta vulgaris*. *Plant Physiol.* 24, 1-15.
- AUDIC, S., CLAVERIE, J.M., 1997: The significance of digital gene expression profiles. *Genome Res.* 7, 986-95.
- ATTARAN, E., MAJOR, I.T., CRUZ, J.A., ROSA, B.A., KOO, A.J.K., CHEN, J., KRAMER, D.M., HE, S.Y., HOWE, G.A., 2014: Temporal dynamics of growth and photosynthesis suppression in response to jasmonate signaling. *Plant Physiol.* 165, 1302-1314.
- BENTON, H.P., IVANISEVIC, J., MAHIEU, N.G., KURCZY, M.E., JOHNSON, C.H., FRANCO, L., RINEHART, D., VALENTINE, E., GOWDA, H., UBHI, B.K., TAUTENHAHN, R., GIESCHEN, A., FIELDS, M.W., PATTI, G.J., SIUZDAK, G., 2015: Autonomous metabolomics for rapid metabolite identification in global profiling. *Anal. Chem.* 87, 884-891.
- BATE, N.J., ROTHSTEIN, S.J., 1998: C₆-volatiles derived from the lipoxygenase pathway induce a subset of defense-related genes. *Plant J.* 16, 561-569.
- CLEVELAND, T.E., CARTER-WIENTJES, C.H., DE LUCCA, A.J., BOUE, S.M., 2009: Effect of soybean volatile compounds on *Aspergillus flavus* growth and aflatoxin production. *J. Food Sci.* 74, 83-87.
- DICKENS, J.C., 1990: Enhancement of insect pheromone responses by green leaf volatiles. *Naturwissenschaften* 77, 29-31.
- ENGELBERTH, J.L., SEIDL-ADAMS, I., SCHULTZ, J.C., TUMLINSON, J.H., 2007: Insect elicitors and exposure to green leafy volatiles differentially upregulate major octadecanoids and transcripts of 12-oxo phytodienoic acid reductases in *Zea mays*. *Mol. Plant Microbe Interact.* 20, 707-716.

- ENGELBERTH, J., CONTRERAS, C.F., DALVI, C., LI, T., ENGELBERTH, M., 2013: Early transcriptome analyses of z-3-hexenol-treated *Zea mays* revealed distinct transcriptional networks and anti-herbivore defense potential of green leaf volatiles. *PLoS One* 8, e77465.
- FROST, C.J., MESCHER, M.C., DERVINIS, C., DAVIS, J.M., CARLSON, J.E., DE MORAES, C.M., 2008: Priming defense genes and metabolites in hybrid poplar by the green leaf volatile, cis-3-hexenyl acetate. *New Phytol.* 180, 722-734.
- GARDNER, H.W., DORNBOS, D.L., DESJARDINS, A.E., 1990: Hexanal, trans-2-Hexenal, trans-2-nonenal inhibit soybean, *Glycine max*, seed germination. *J. Agr. Food Chem.* 38, 1316-1320.
- GOMI, K., YAMASKI, Y., YAMAMOTO, H., AKIMITSU, K., 2003: Characterization of a hydroperoxide lyase gene and effect of C₆-volatiles on expression of genes of the oxylipin metabolism in *Citrus*. *J. Plant Physiol.* 160, 1219-1231.
- HIRAO, T., OKAZAWA, A., HARADA, K., KOBAYASHI, A., MURANAKA, T., HIRATA, K., 2012: Green leaf volatiles enhance methyl jasmonate response in *Arabidopsis*. *J. Biosci. Bioeng.* 114, 540-545.
- JUNG, S., 2004: Effect of chlorophyll reduction in *Arabidopsis thaliana* by methyl jasmonate or norflurazon on antioxidant systems. *Plant Physiol. Biochem.* 42, 225-231.
- KISHIMOTO, K., MATSUI, K., OZAWA, R., TAKABAYASHI, J., 2005: Volatile C₆-aldehydes and allo-ocimene activate defense genes and induce resistance against *Botrytis cinerea* in *Arabidopsis thaliana*. *Plant Cell Physiol.* 46, 1093-1102.
- KISHIMOTO, K., MATSUI, K., OZAWA, R., TAKABAYASHI, J., 2006: ETR-, JAR1- and PAD2-dependent signaling pathways are involved in C₆-aldehyde-induced defense responses of *Arabidopsis*. *Plant Sci.* 171, 415-423.
- LI, B., DEWEY, C.N., 2011: RSEM: accurate transcript quantification from RNA-Seq data with or without a reference genome. *BMC Bioinformatics* 12, 323.
- LIU, M., LI, P., ZENG, X., WU, H., SU, W., HE, J., 2015: Identification and pharmacokinetic of multiple potential bioactive constituents after oral administration of *Radix Astragali* on cyclophosphamide-induced immunosuppression in Balb/c Mice. *Int. J. Mol. Sci.* 16, 5047-5071.
- LIU, J., YANG, H., ZHU, X., ZHAO, Z., CHEN, H., 2011: Comparative study of wild and cultivated astragali radix in Daqingshan district in Wuchuan of Neimenggu. *Zhongguo Zhong Yao Za Zhi* 36, 1577-1581.
- MARTIN, M., 2011: Cutadapt removes adapter sequences from high-throughput sequencing reads. *EMBnet Journal* 7, 10-12.
- MOSES, T., PAPADOPOULOU, K.K., OSBOURN, A., 2014: Metabolic and functional diversity of saponins, biosynthetic intermediates and semi-synthetic derivatives. *Crit. Rev. Biochem. Mol. Biol.* 49, 439-462.
- PAN, H., FANG, C., ZHOU, T., WANG, Q., CHEN, J., 2007: Accumulation of calycosin and its 7-O-beta-D-glucoside and related gene expression in seedlings of *Astragalus membranaceus* Bge. var. *mongholicus* (Bge.) Hsiao induced by low temperature stress. *Plant Cell Rep.* 26, 1111-1120.
- SCHUMAN, M.C., BARTHEL, K., BALDWIN, I.T., 2012: Herbivory-induced volatiles function as defenses increasing fitness of the native plant *Nicotiana attenuata* in nature. *eLife* 1, e00007.
- SONG, Z.H., JI, Z.N., LO, C.K., DONG, T.T., ZHAO, K.J., LI, O.T., HAINES, C.J., KUNG, S.D., TSIM, K.W., 2014: Chemical and biological assessment of a traditional Chinese herbal decoction prepared from *Radix Astragali* and *Radix Angelicae Sinensis*: Orthogonal array design to optimize the extraction of chemical constituents. *Planta Med.* 70, 1222-1227.
- SUN, H., WANG, W., HAN, P., SHAO, M., SONG, G., DU, H., YI, T., LI, S., 2016: Astragaloside IV ameliorates renal injury in db/db mice. *Sci. Rep.* 6, e32545.
- SUN, H., XIE, D., GUO, X., ZHANG, L., LI, Z., WU, B., QIN, X., 2010: The study on the relevance between beany flavor and main bioactive components in *Radix Astragali*. *J. Agric. Food Chem.* 58, 5568-5573.
- UL HASSAN, M.N., ZAINAL, Z., ISMAIL, I., 2015: Green leaf volatiles: biosynthesis, biological functions and their applications in biotechnology. *Plant Biotechnol. J.* 13, 727-39.
- WASTERACK, C., HAUSE, B., 2013: Jasmonates: biosynthesis, perception, signal transduction and action in plant stress response, growth and development. An update to the 2007 review in *Annals of Botany*. *Ann. Bot.* 111, 1021-1058.
- YAN, Z., WANG, C., 2006: Wound-induced green leaf volatiles cause the release of acetylated derivatives and a terpenoid in maize. *Phytochemistry* 67, 34-42.
- YAMAUCHI, Y.L., KUNISHIMA, M.L., MIZUTANI, M.L., SUGIMOTO, Y.L., 2015: Reactive short-chain leaf volatiles act as powerful inducers of abiotic stress-related gene expression. *Sci. Rep.* 5, e8030.
- ZERINGUE, H.J., 1992: Effects of C₆-C₁₀ alkenals and alkanals on eliciting a defence response in the developing cotton boll. *Phytochemistry* 31, 2305-2308.
- ZHAO, C., ZENG, Y., WAN, M., LI, R., LIANG, Y., LI, C., ZENG, Z., CHAU, F.T., 2009: Comparative analysis of essential oils from eight herbal medicines with pungent flavor and cool nature by GC-MS and chemometric resolution methods. *J. Sep. Sci.* 32, 660-670.
- ZHU, G., YE, N., YANG, J., PENG, X., ZHANG, J., 2011: Regulation of expression of starch synthesis genes by ethylene and ABA in relation to the development of rice inferior and superior spikelets. *J. Exp. Bot.* 62, 3907-3916.

Address of the authors:

Dr. Sun Haifeng, MSc Kang Baoling, College of Chemistry and Chemical Engineering, Shanxi University, No.92, Wuchenglu, Taiyuan 030006, China
E-mail: haifeng@sxu.edu.cn

Prof. Dr. Guo Lanping, Dr. Kang Liping, State Key Laboratory Breeding Base of Dao-di Herbs, National Resource Center of Chinese Materia Medica, China Academy of Chinese Medical Sciences, No. 16, Nanxiaojie, Dongzhimen, Dongcheng District, Beijing 100700, China
E-mail: glp01@126.com

MSc Sun Huanhuan, Prof. Dr. Gao Jianping, College of Pharmacy, Shanxi Medical University, No.56, Xinjiannanlu, Taiyuan 030001, China
E-mail: jgao123@163.com

© The Author(s) 2017.

 This is an Open Access article distributed under the terms of the Creative Commons Attribution Share-Alike License (<http://creativecommons.org/licenses/by-sa/4.0/>).

Tab. S1: Seasonal changes of the hexanal level in fresh roots of 2-year old *Astragalus membranaceus* var. *mongholicus* plants during a phenological period. The result was obtained from 6 plant species distributed in 2 subpopulation of Hunyuan, Shanxi, China. Superscript marked with different letters indicates significant differences in the concentration.

Collection time	Concentration ($\mu\text{g/g}$)	Concentration ($\mu\text{mol/g}$)
Vegatative stage	330.3 \pm 10.1 ^a	3.3 \pm 0.1 ^a
Flowering stage	499.5 \pm 54.2 ^a	5.0 \pm 0.5 ^a
Seed maturity stage	531.7 \pm 31.8 ^a	5.3 \pm 0.3 ^a
Traditional harvest stage	1897.0 \pm 370.6 ^b	18.9 \pm 3.7 ^b

Tab. S2: Retention time and MS data of flavonoids and saponins identified in *Astragalus membranaceus* var. *mongholicus* seedling roots and leaves

No.	Identification	Formula	T_R (min)	$[M+Na]^+ / [M+H]^+$ (m/Z)	Other fragment ions (m/z)
1	Acetyl-(6aR,11aR)-3,9-dimethoxy-10-hydroxypterocarpan	$C_{19}H_{18}O_6$	0.49	365.1034 343.1277	377.0851[M+Cl] ⁻ , 341.1084 [M-H] ⁻ , 323.0754[M-H-H ₂ O] ⁻ , 325.1118[M+H-H ₂ O] ⁺ , 381.0775[M+K] ⁺ , 475.1765[M+H+Xyl] ⁺ , 458.1852[M+H-2H+Xyl-CH ₃] ⁻
2	(6aR,11aR)-3,9,10-trinethoxypterocarpan	$C_{18}H_{18}O_5$	4.34	315.0853	354.2627[M+K] ⁺ , 313.0728[M-H] ⁻ , 299.0469[M-CH ₃], 301.1077[M+H-CH ₃] ⁺ , 284.0698[M-2CH ₃], 269.0833[M-3CH ₃], 345.2281[M-H+2H+HCOO] ⁺
3	Isomucronulatol 7-O-glucoside	$C_{23}H_{28}O_{10}$	3.99	487.1554 465.1745	463.1598[M-H] ⁻ , 509.1657[M+HCOO] ⁻ , 303.1216[M+H-Glc] ⁺ , 301.1067[M-H-Glc] ⁻ , 482.2019[M+NH ₄] ⁺
4	9,10-dimethoxypterocarpan-7-O-β-D-glucopyranoside	$C_{23}H_{26}O_{10}$	3.82	485.1588 463.1835	301.1619[M+H-Glc] ⁺ , 507.1485[M+HCOO] ⁻ , 779.1085[2M+NH ₃ -Glc] ⁺
5	Pratensein-7-O-β-D-glucoside	$C_{22}H_{22}O_{11}$	4.27	485.1227 463.1438	461.1066[M-H] ⁻ , 507.1157[M+HCOO] ⁻ , 301.1264[M+H-Glc] ⁺ , 947.0925[2M+Na] ⁺ , 301.1264[M+H-Glc] ⁺ , 517.1348[M+H+3H ₂ O] ⁺ , 524.0995[M+H ₂ O+HCOO] ⁻
6	(3R)-8, 2'-dihydroxy-7,4-dimethoxyisoflavan	$C_{17}H_{18}O_5$	1.52	303.2019	301.1874[M-H] ⁻ , 285.0585[M-OH] ⁻
7	Calycosin	$C_{16}H_{12}O_5$	4.12	285.0747	283.0602[M-H] ⁻ , 270.0524[M+H-CH ₃] ⁺ , 268.0398[M-H-CH ₃] ⁻
8	Calycosin-7-O-β-D-glucoside	$C_{22}H_{22}O_{10}$	2.29	469.1094 447.1273	285.0753[M+H-Glc] ⁺ , 491.1187[M+HCOO] ⁻ , 283.0593[M-H-Glc] ⁻ , 446.1201[M]
9	Astragalin (Kaempferol 3-O-β-D-glucoside)	$C_{21}H_{20}O_{11}$	2.71	471.1103 449.1341	447.0887[M-H] ⁻ , 287.1130[M+H-Glc] ⁺ , 285.0896[M-H-Glc] ⁻ , 919.0762[2M+Na] ⁺
10	Isoquercitroside	$C_{21}H_{20}O_{12}$	2.36	487.0844 465.1024	463.0872[M-H] ⁻ , 303.0490[M+H-Glc] ⁺ , 579.1347[M-H+CO ₂ +4H ₂ O] ⁻
11	Isorhamnetin-3-O-glucoside	$C_{22}H_{22}O_{12}$	2.81	501.1002 479.1183	477.1034[M-H] ⁻ , 317.0648[M+H-Glc] ⁺
12	Malonylramnocitrin-3-O-β-D-glucoside	$C_{25}H_{24}O_{14}$	4.53	571.1016 549.1245	503.1186[M-COOH] ⁻ , 548.1113[M], 301.1264[M-Mal-Glc-H] ⁻ , 1095.2227[2M-H] ⁻ , 1119.0365[2M+Na] ⁺
13	Isoliquiritigenin	$C_{15}H_{12}O_4$	3.54	257.2241	343.2119[M+2H ₂ O+Cl] ⁻
14	Formononetin	$C_{16}H_{12}O_4$	5.76	269.0799	267.0653[M-H] ⁻ , 351.2130[M+CO ₂ +K] ⁺ , 252.0447[M-H-CH ₃] ⁻
15	Ononin	$C_{22}H_{22}O_9$	3.47	453.1151 431.1332	475.1235[M+HCOO] ⁻ , 269.0803[M+H-Glc] ⁺ , 267.0653[M-H-Glc] ⁻ , 883.2443[2M+Na] ⁺
16	Formononetin-7-O-β-D-Glu-6"-O-malonate	$C_{25}H_{24}O_{12}$	3.67	539.2468 517.2647	515.2485[M-H] ⁻ , 269.0811[M+H-Mal-Glc] ⁺ , 267.0696[M-H-Mal-Glc] ⁻ , 252.0452[M-H-Mal-Glc-CH ₃] ⁻
17	2R-farrerol-7-O-β-D-glucoside	$C_{23}H_{26}O_{10}$	3.85	485.1418 463.1591	507.1507[M+HCOO] ⁻ , 301.1061[M+H-Glc] ⁺ , 947.2927[2M+Na] ⁺ , 299.0906[M-H-Glc] ⁻
18	7-Hydroxyflavan	$C_{15}H_{14}O_2$	1.82	227.2413	225.1591[M-H] ⁻ , 209.2324[M-OH] ⁻
19	Cycloastragenol 3-O-β-D-glucoside	$C_{36}H_{60}O_{10}$	4.08	675.3718	697.4109[M+HCOO] ⁻ , 714.3990[M+HCOO+NH ₃] ⁻ , 635.3903[M-H ₂ O+H] ⁺ , 617.3895[M-2H ₂ O+H] ⁺ , 599.3648[M-3H ₂ O+H] ⁺ , 473.3862[M-Glc-H ₂ O+H] ⁺ , 437.3690[M-Glc-3H ₂ O+H] ⁺ , 419.3605[M-Glc-4H ₂ O+H] ⁺ , 401.3576[M-Glc-4H ₂ O+H] ⁺ , 1327.5717[2M+Na] ⁺

20	Mongholicoside I	C ₃₆ H ₆₀ O ₉	5.7	659.4124	675.4028[M+K] ⁺ , 681.4200[M+HCOO] ⁻
21	Isoastragaloside IV	C ₄₁ H ₆₈ O ₁₄	5.92	785.4667,	829.4560[M+HCOO] ⁻ , 767.4590[M+H-H ₂ O] ⁺ , 749.4473[M+H-2H ₂ O] ⁺ ,
	807.4517			605.4053[M+H-Glc] ⁺ , 587.3948[M+H-Glc-H ₂ O] ⁺ , 819.4296[M+Cl] ⁻ , 803.4482[M+H+H ₂ O] ⁺	
22	Astragaloside IV	C ₄₁ H ₆₈ O ₁₄	5.98	807.4496	587.3924[M+H-Glc-H ₂ O] ⁺ , 829.4570[M+HCOO] ⁻ , 473.3622[M+H-Glc-Xyl-H ₂ O] ⁺
	Astragaloside II			C ₄₃ H ₇₀ O ₁₅	4.9
23	Isoastragaloside II	C ₄₃ H ₇₀ O ₁₅	6.3	827.4798,	871.4668[M+HCOO] ⁻ , 825.4622[M-H] ⁻ , 647.4158[M+H-Glc-H ₂ O] ⁺
	849.4588				
23	Malonylastragaloside IV	C ₄₄ H ₆₉ O ₁₇	6.91	891.4744	913.4780[M+HCOO] ⁻
24	Methylastragaloside II	C ₄₄ H ₇₃ O ₁₆	5.36	857.2159,	855.1957[M-H] ⁻ , 901.4769[M+HCOO] ⁻ , 825.1848[M-H-CH ₂ O] ⁻ ,
				879.4698	781.1943[M-H-CH ₂ O-CO ₂] ⁻
25	Soyasaponin I	C ₄₈ H ₇₈ O ₁₈	6.25	943.5259, 962.4933	941.5085[M-H] ⁻ , 987.5140[M+HCOO] ⁻
26	Malonylastragaloside I	C ₄₈ H ₇₃ O ₁₉	7.05	977.4719,	953.4738[M-H] ⁻ , 937.48.5[M+H-H ₂ O] ⁺ , 891.4717[M-Mal+Na] ⁺
				955.4902	
27	Cyclocanthoside E	C ₄₁ H ₇₀ O ₁₄	3.40	809.1912	749.1705[M+H-2H ₂ O] ⁺ , 785.1912[M-H] ⁻
28	Huangqiyein D	C ₃₈ H ₆₂ O ₁₁	3.95	695.1828,	693.1662[M-H] ⁻ , 649.1768[M+HCOO-5H ₂ O] ⁻ , 533.1293[M+H-Glc] ⁺
				717.1650	
29	Mongholicoside II	C ₃₈ H ₆₂ O ₁₁	6.04	717.4181	739.4254[M+HCOO] ⁻ , 1411.8480[2M+Na] ⁺ , 659.4169[M+H-2H ₂ O] ⁺ , 497.3625[M+H-2H ₂ O-Glc] ⁺ , 479.3517[M+H-3H ₂ O-Glc] ⁺

Tab. S3: Representative compounds derived from fatty acid metabolism with fluctuant levels following treatment with 50 μ M hexanal

T_R /mi	Chemical name	Formula	z/m	MW	PPM	KEGG/LMID ID	Tissue
3.23	Ethyl (S)-3-hydroxybutyrate glucoside*	C ₁₂ H ₂₂ O ₈	317.121	294.1315	2		Leaf
3.98	3-Oxododecanoic acid glycerides	C ₁₅ H ₂₉ O ₆	390.284	305.1964	1		Leaf
5.00	11,12-dihydroxy arachidic acid*	C ₂₀ H ₄₀ O ₄	367.282	344.2926	0	LMFA01050095	Leaf
10.59	18:1 Stigmasteryl ester*	C ₄₇ H ₈₀ O ₂	711.585	676.6158	1	LMST01020064	Leaf
6.03	9-hexadecen-1-ol	C ₁₆ H ₃₂ O	279.209	240.2453	3		Leaf
1.35	O-propanoyl-carnitine*	C ₁₀ H ₁₉ NO ₄	218.138	217.1314	4	C03017/HMDB00824	Root
1.87	2-tridecene-4,7-diyndal	C ₁₃ H ₁₆ O	189.127	188.1201	4	LMFA06000077	Leaf
3.20	Norselic acid E	C ₃₁ H ₄₂ O ₅	533.264	494.3032	4	LMST01040190	Leaf
6.71	Umbelliferyl Arachidonate*	C ₂₉ H ₃₆ O ₄	471.253	448.2614	0		Root
5.73	DG (20:5(5Z,8Z,11Z,14Z,17Z))	C ₄₅ H ₇₀ O ₅	725.493	690.5223	2	LMGL02010274	Leaf
6.95	PA (P-16:0/12:0)*	C ₃₁ H ₆₁ O ₇ P	577.422	576.4155	2		Root
6.32	PA (P-20:0/0:0)*	C ₂₃ H ₄₇ O ₆ P	451.32	450.3110	4	LMGP10070001	Leaf
6.05	PA (O-18:0/14:0)	C ₃₅ H ₇₁ O ₇ P	721.421	634.4937	0	LMGP10020021	Leaf
5.53	PA (14:0/14:0)[U]	C ₃₁ H ₆₁ O ₈ P	627.375	592.4104	8	LMGP10010010	Leaf
5.60	TG (20:4(5Z,8Z,11Z,14Z))	C ₆₁ H ₉₃ D ₅ O ₆	959.689	921.6972	1	LMGL03010016	Leaf
10.11	PC (25:0/26:0)*	C ₅₉ H ₁₁₈ NO ₈ P	1034.834	999.8595	5		Root
9.36	PC (O-18:0/22:0)*	C ₄₈ H ₉₈ NO ₇ P	870.664	831.7081	9	LMGP01020105	Leaf
10.95	PC (14:1(9Z)/22:6(4Z,7Z,10Z,13Z,16Z,19Z))	C ₄₄ H ₇₄ NO ₈ P	814.485	775.5152	9	C00157	Leaf
5.60	PI (13:0/18:3(6Z,9Z,12Z))	C ₄₀ H ₇₁ O ₁₃ P	791.474	790.4632	5	LMGP06010047	Leaf
9.96	PI (O-16:0/17:2(9Z,12Z))	C ₄₂ H ₇₉ O ₁₂ P	829.522	806.5309	2	LMGP06020010	Leaf
11.76	PG (18:3(6Z,9Z,12Z)/20:5(5Z,8Z,11Z,14Z,17Z))	C ₄₄ H ₇₁ O ₁₀ P	813.472	790.4785	5	LMGP04010390	Leaf
5.84	PG (22:4(7Z,10Z,13Z,16Z)/0:0)	C ₂₈ H ₄₉ O ₉ P	559.304	560.3114	0	LMGP04050017	Leaf
5.77	PIP (16:0/20:4(5Z,8Z,11Z,14Z))	C ₄₅ H ₈₀ O ₁₆ P ₂	939.507	938.4922	8	HMDB09931	Leaf
5.94	PS (19:0/22:1(11Z))	C ₄₇ H ₉₀ NO ₁₀ P	894.596	859.6302	4	LMGP03010476	Leaf

Superscript star on the top-right of the compounds denotes the significant decrease in the concentration.

Tab. S4: Annotation of metabolites derived from lipids

Name	M/Z	Id	Match_Form	Mz_Difference
3-oxomyrist-7-enoyl-CoA	494.1273	CE0782	M(C13)+2H[2+]	-0.0046
	942.2658	CE0782	M-CO ₂ +H[1+]	0.0024
	950.2381	CE0782	M-H ₄ O ₂ +H[1+]	0.0061
Hexadecanoic acid	325.2363	C00249	M+HCOONa[1+]	0.0014
	325.2373	C00249	M+HCOONa[1+]	0.0024
	279.231	C00249	M+Na[1+]	0.0015
	279.2309	C00249	M+Na[1+]	0.0014
	279.2311	C00249	M+Na[1+]	0.0016
Octadecanoic acid	353.2673	C01530	M+HCOONa[1+]	0.0011
	353.269	C01530	M+HCOONa[1+]	0.0028
	353.2672	C01530	M+HCOONa[1+]	0.001
	307.2622	C01530	M+Na[1+]	0.0014
	307.2605	C01530	M+Na[1+]	-0.0003
	369.2414	C01530	M+HCOOK[1+]	0.0013
	307.2634	C01530	M+Na[1+]	0.0026
4-Hydroxy-5-phenyltetrahydro-1,3-oxazin -2-one	150.091	C16595	M-CO ₂ +H[1+]	-0.0004
Acetyl-CoA	812.1365	C00024	M(C137)+H[1+]	0.0062
	811.1359	C00024	M(C13)+H[1+]	-0.0006
	812.1228	C00024	M(S34)+H[1+]	-0.0061
	811.1353	C00024	M(C13)+H[1+]	-0.0012
	405.5712	C00024	M+2H[2+]	0.001
	812.1228	C00024	M(C137)+H[1+]	-0.0075
	828.1487	C00024	M+H ₂ O+H[1+]	0.005
	812.1365	C00024	M(S34)+H[1+]	0.0076
	766.1414	C00024	M-CO ₂ +H[1+]	-0.0019
	793.1058	C00024	M-NH ₃ +H[1+]	-0.0008
	811.1288	C00024	M(C13)+H[1+]	-0.0077
810.129	C00024	M+H[1+]	-0.0041	
3,4-Dihydroxymandelaldehyde	97.0284	C05577	M-C ₃ H ₄ O ₂ +H[1+]	-0.0001
	123.0432	C05577	M-HCOOH+H[1+]	-0.001
	123.0431	C05577	M-HCOOH+H[1+]	-0.0011
	169.0491	C05577	M+H[1+]	-0.0005
2-Methylacetoacetyl-CoA	838.1725	C03344	M-CO+H[1+]	0.0082
	782.2011	C03344	M-HCOOK+H[1+]	0.0031
	865.144	C03344	M[1+]	-0.008
	865.1598	C03344	M[1+]	0.0078
	866.1608	C03344	M+H[1+]	0.0015

(S)-Hydroxyhexanoyl-CoA	865.1598	C05268	M-NH ₃ +H[1+]	-0.0043
	865.1598	C05268	M-NH ₃ +H[1+]	-0.0043
	881.1886	C05268	M[1+]	0.0053
	814.1972	C05268	M-HCOONa+H[1+]	-0.006
	814.2099	C05268	M-HCOONa+H[1+]	0.0067
	884.1789	C05268	M(S34)+H[1+]	-0.0075
	882.1819	C05268	M+H[1+]	-0.0087
	854.1939	C05268	M-CO+H[1+]	-0.0017
	882.1949	C05268	M+H[1+]	0.0043
	882.1915	C05268	M+H[1+]	0.0009
	836.1883	C05268	M-HCOOH+H[1+]	0.0031
	838.1962	C05268	M-CO ₂ +H[1+]	-0.0046
	846.1767	C05268	M-H ₄ O ₂ +H[1+]	0.0073
3-Oxodecanoyl-CoA	852.2679	C05265	M-HCOOK+H[1+]	-0.0083
	852.2756	C05265	M-HCOOK+H[1+]	-0.0006
cis-6-dodecenoyl-CoA	860.2875	CE4794	M-HCOOK+H[1+]	0.0062
	945.2392	CE4794	M(C13)+H[1+]	-0.0068
	962.2558	CE4794	M+H ₂ O+H[1+]	0.0026
2(S),6-dimethyl-heptanoyl-CoA	887.1822	CE4798	M-NH ₃ +H[1+]	-0.0026
	302.0731	CE4798	M+3H[3+]	-0.0022
	302.0729	CE4798	M+3H[3+]	-0.0024
	905.2153	CE4798	M(C13)+H[1+]	0.0006
	988.1736	CE4798	M+HCOOK[1+]	0.001
	302.0726	CE4798	M+3H[3+]	-0.0027
	836.2187	CE4798	M-HCOONa+H[1+]	-0.0052
	302.0723	CE4798	M+3H[3+]	-0.003
	860.2223	CE4798	M-CO ₂ +H[1+]	0.0008
	302.0732	CE4798	M+3H[3+]	-0.0021
	905.2216	CE4798	M(C13)+H[1+]	0.0069
860.2133	CE4798	M-CO ₂ +H[1+]	-0.0082	
(2E)-Hexenoyl-CoA	836.1883	C05271	M-CO+H[1+]	0.0033
	846.1767	C05271	M-H ₂ O+H[1+]	0.0073
	882.1819	C05271	M+H ₂ O+H[1+]	-0.0087
	865.181	C05271	M(C13)+H[1+]	-0.0024
	882.1915	C05271	M+H ₂ O+H[1+]	0.0009
	866.1724	C05271	M(C137)+H[1+]	-0.0048
	865.1912	C05271	M(C13)+H[1+]	0.0078
	289.068	C05271	M(C13)+3H[3+]	0.0021
	866.1724	C05271	M(S34)+H[1+]	-0.0034
	882.1949	C05271	M+H ₂ O+H[1+]	0.0043
	796.1944	C05271	M-HCOONa+H[1+]	0.0018
Decanoyl-CoA	850.2293	C05274	M-C ₃ H ₄ O ₂ +H[1+]	-0.0079
	886.2296	C05274	M-H ₄ O ₂ +H[1+]	-0.0075

	308.0929	C05274	M+3H[3+]	0.002
3-oxo-cis-8-tetradecenoyl-CoA	494.1273	CE4792	M(C13)+2H[2+]	-0.0046
	942.2658	CE4792	M-CO ₂ +H[1+]	0.0024
	950.2381	CE4792	M-H ₄ O ₂ +H[1+]	0.0061
2(R),6-dimethyl-heptanoyl-CoA	887.1822	CE4797	M-NH ₃ +H[1+]	-0.0026
	302.0731	CE4797	M+3H[3+]	-0.0022
	302.0729	CE4797	M+3H[3+]	-0.0024
	905.2153	CE4797	M(C13)+H[1+]	0.0006
	988.1736	CE4797	M+HCOOK[1+]	0.001
	302.0726	CE4797	M+3H[3+]	-0.0027
	836.2187	CE4797	M-HCOONa+H[1+]	-0.0052
	302.0723	CE4797	M+3H[3+]	-0.003
	860.2223	CE4797	M-CO ₂ +H[1+]	0.0008
	302.0732	CE4797	M+3H[3+]	-0.0021
	905.2216	CE4797	M(C13)+H[1+]	0.0069
	860.2133	CE4797	M-CO ₂ +H[1+]	-0.0082
cis-laur-5-enoyl-CoA	860.2875	CE0695	M-HCOOK+H[1+]	0.0062
	945.2392	CE0695	M(C13)+H[1+]	-0.0068
	962.2558	CE0695	M+H ₂ O+H[1+]	0.0026
(9Z,12Z,15Z)-Octadecatrienoic acid	280.2341	C06427	M(C13)+H[1+]	-0.0012
	279.231	C06427	M+H[1+]	-0.0009
	280.2379	C06427	M(C13)+H[1+]	0.0026
	151.1118	C06427	M+H+Na[2+]	0.0012
	347.2181	C06427	M+HCOONa[1+]	-0.0012
	207.2113	C06427	M-C ₃ H ₄ O ₂ +H[1+]	0.0005
	261.2204	C06427	M-H ₂ O+H[1+]	-0.0009
	337.1888	C06427	M+NaCl[1+]	-0.0017
	151.1115	C06427	M+H+Na[2+]	0.0009
	347.221	C06427	M+HCOONa[1+]	0.0017
	243.2101	C06427	M-H ₄ O ₂ +H[1+]	-0.0006
	261.2234	C06427	M-H ₂ O+H[1+]	0.0021
	279.2311	C06427	M+H[1+]	-0.0008
	279.2309	C06427	M+H[1+]	-0.001
(6Z,9Z,12Z)-Octadecatrienoic acid	280.2341	C06426	M(C13)+H[1+]	-0.0012
	279.231	C06426	M+H[1+]	-0.0009
	280.2379	C06426	M(C13)+H[1+]	0.0026
	151.1118	C06426	M+H+Na[2+]	0.0012
	347.2181	C06426	M+HCOONa[1+]	-0.0012
	207.2113	C06426	M-C ₃ H ₄ O ₂ +H[1+]	0.0005
	261.2204	C06426	M-H ₂ O+H[1+]	-0.0009
	337.1888	C06426	M+NaCl[1+]	-0.0017
	151.1115	C06426	M+H+Na[2+]	0.0009
	347.221	C06426	M+HCOONa[1+]	0.0017
	243.2101	C06426	M-H ₄ O ₂ +H[1+]	-0.0006
	261.2234	C06426	M-H ₂ O+H[1+]	0.0021
	279.2311	C06426	M+H[1+]	-0.0008
	279.2309	C06426	M+H[1+]	-0.001

All-Unigene GO Classification

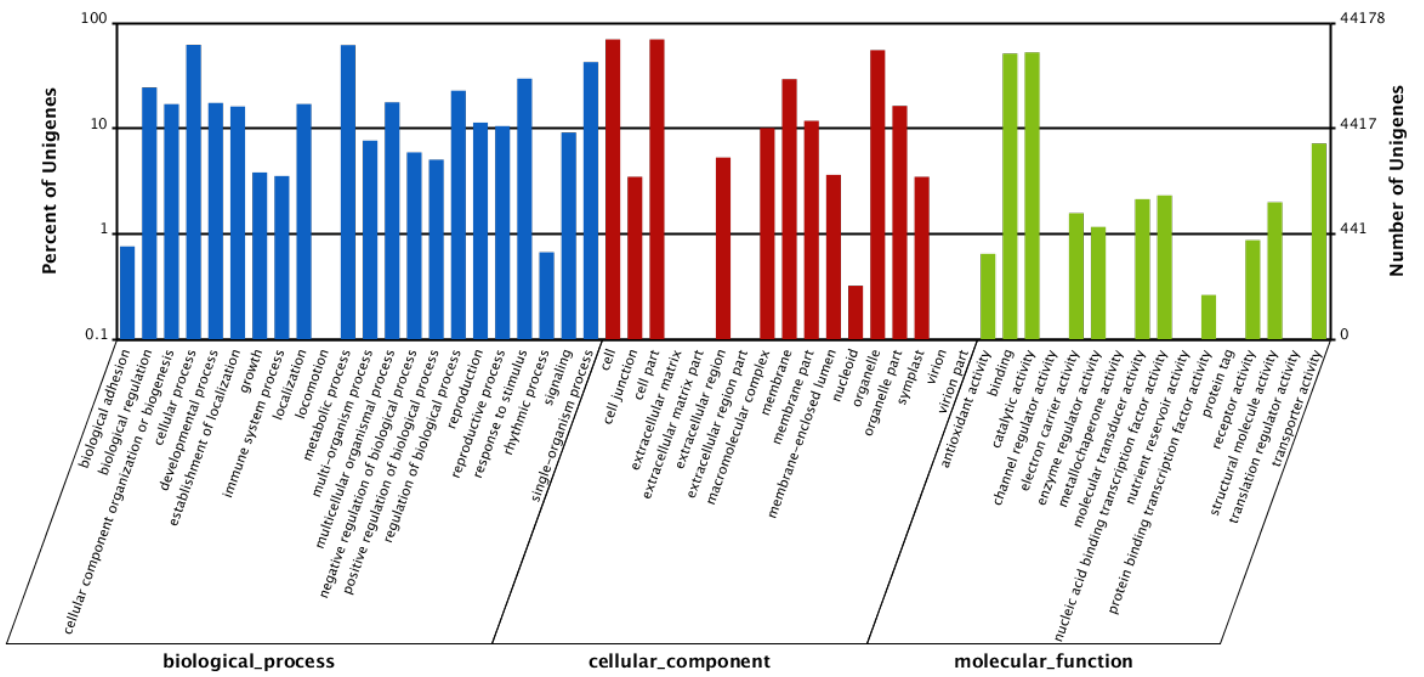


Fig. S1 GO annotation of All-Unigenes.